Capillary rise of a liquid between two vertical plates making a small angle

F. J. Higuera,[1] A. Medina,[2] and A. Liñán[1]
[1]*E. T. S. Ingenieros Aeronáuticos, UPM, Plaza Cardenal Cisneros 3, 28040 Madrid, Spain*
[2]*SEPI-ESIME-A. Instituto Politécnico Nacional, Av. de las Granjas 682, Col. Sta. Catarina Azcapotzalco, Mexico DF 02550, Mexico*

(Received 30 May 2008; accepted 24 September 2008; published online 20 October 2008)

The penetration of a wetting liquid in the narrow gap between two vertical plates making a small angle is analyzed in the framework of the lubrication approximation. At the beginning of the process, the liquid rises independently at different distances from the line of intersection of the plates except in a small region around this line where the effect of the gravity is negligible. The maximum height of the liquid initially increases as the cubic root of time and is attained at a point that reaches the line of intersection only after a certain time. At later times, the motion of the liquid is confined to a thin layer around the line of intersection whose height increases as the cubic root of time and whose thickness decreases as the inverse of the cubic root of time. The evolution of the liquid surface is computed numerically and compared with the results of a simple experiment.
 [DOI: 10.1063/1.3000425]

I. INTRODUCTION

Capillary flows in confined liquid films arise in numerous contexts, including flows in porous media, microfluidics, fluid management in low gravity environments, and the wetting and spreading of liquids on irregular surfaces; see, e.g., Kistler[1] and Steen.[2] Interior corners in the solid wall of a channel or a container partially filled with a wetting liquid enhance capillary effects by increasing the local curvature of the liquid surface in order to satisfy the contact angle wetting condition. As early as 1712, Taylor[3] and Hauksbee[4] reported investigations on the shape of the equilibrium meniscus in the gap between two vertical plates making a small angle, showing that the equilibrium contact line is a hyperbola. Static menisci at interior corners have been studied subsequently by Concus and Finn,[5] Mason and Morrow,[6] Langbein,[7] and Wong *et al.*,[8] among others.

Analysis of the imbibition of a wetting liquid in the corners of a noncircular capillary tube is of interest to ascertain the mechanisms of spreading, the capillary instability leading to snap off of threads of a nonwetting phase, and the displacement and trapping of this phase. Applications range from wetting of powders[9] to oil recovery[10] and oil spills in unsaturated soils[11] and from biophysics[12–15] to environmental[16] and agriculture[17] problems. Lenormand and Zarcone[18] computed the flow along a corner using a hydraulic diameter approximation. Ayyaswamy *et al.*[19] and Ransohoff and Radke[20] solved the problem under the assumptions that the flow of the advancing liquid is quasiunidirectional and with negligible inertial effects. The evolution of the liquid obeys then a nonlinear convection-diffusion equation whose coefficients depend on a friction factor or dimensionless flow resistance that measures the hydraulic resistance of the walls to the flow and has been expressed and computed in various manners. Dong and Chatzis[21] used this formulation to analyze the imbibition of a liquid in the corners of a capillary tube of square cross section and found a similarity solution of the governing equation applicable to their problem. Other solutions and comparisons to drop tower low gravity experiments have been reported by Weislogel and Lichter.[22,23] Modifications of the governing equation to account for a gravity force opposing spreading have been discussed by Verbist *et al.*[24] and Kovscek and Radke.[25] Ma *et al.*[26] first tried to account for a liquid-gas frictional interaction in their analysis of the flow in triangular microgrooves, a work that was continued and applied to the analysis of the heat transfer in microheat pipes in Refs. 27–30 and complemented and improved by Su and Lai,[31] who removed an arbitrary assumption on the velocity at the surface originally made to simplify the computation of the friction factor. Kolb and Cerro[32] and Bico and Quéré[33] investigated the motion of long bubbles in angular capillary tubes. Weislogel[34] provided a collection of solutions for capillary driven flows in interior corners of interest for low gravity applications. See Refs. 35–37 for other investigations on capillary flows in V-shaped grooves.

The simple configuration of the pioneering works of Taylor[3] and Hauksbee,[4] with two vertical plates making a small angle, is revisited in this paper to analyze the capillary rise of a viscous wetting liquid in the narrow gap between the plates. A free boundary problem is formulated in the framework of the lubrication approximation for the flow in the gap, assuming that inertial effects are negligible. A self-similar solution of this problem is computed in the absence of gravity, which is applicable to the early stages of the process in a region around the edge of the gap where the two plates intersect. This solution predicts that the height of the liquid is minimum at the edge and increases linearly with time. The effect of the gravity is first felt far from the edge, leading to a distribution of liquid height that reaches a maximum at a certain point and tends toward the equilibrium hyperbola further away from the edge. The point of maximum height shifts toward the edge as time increases and reaches the edge in a finite time. A thin layer develops around the edge at later times, whose evolution can be de-

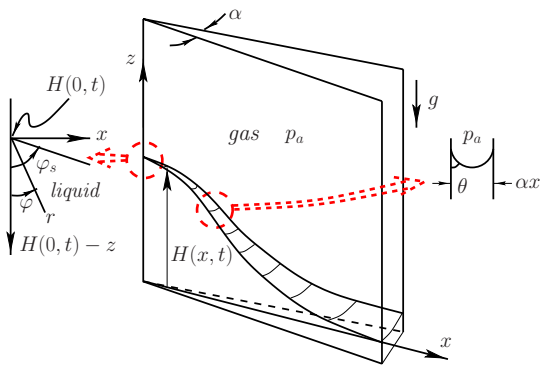

FIG. 1. (Color online) Definition sketch.

scribed by a convection-diffusion equation similar to that used in the analysis of the flow in corners of nonsmall angles but with closed form coefficients. The numerical results are compared with experiments carried out with silicone oil rising between two glass plates.

II. FORMULATION

The wedge-shaped gap between two vertical plates intersecting at an angle $\alpha \ll 1$ is initially empty. At a certain time, the lower edges of the plates are brought in contact with a liquid of density ρ, viscosity μ, and surface tension σ. The liquid wets the plates with a contact angle $\theta < \pi/2$ and therefore rises between the plates by capillary action,[5] as sketched in Fig. 1. The ratio of the two principal curvatures of the free surface of the liquid between the plates is small, of the order of α. The normal section of maximum curvature, by a plane nearly normal to the plates, is approximately an arc of circle of radius $\alpha x/2\cos\theta$, where x is the distance to the line of intersection of the plates (see sketch on the right-hand side of Fig. 1). The pressure jump across the surface is approximately $\Delta p_s = 2\sigma\cos\theta/\alpha x$. At equilibrium, the height $H_e(x)$ of the meniscus above the level of the outer liquid is determined by the balance $\Delta p_s = \rho g H_e$, where g is the acceleration due to gravity. This balance gives the rectangular hyperbola[3,4]

$$H_e = \frac{H_c^2}{x} \quad \text{with} \quad H_c = \left(\frac{2\sigma\cos\theta}{\rho g\alpha}\right)^{1/2}. \tag{1}$$

This well known result needs be corrected at distances from the line of intersection of the plates of the order of $H_c/\alpha^{1/2}$, where the elevation of the liquid surface and the distance between the plates are of the order of the capillary length of the liquid, $\alpha^{1/2}H_c$, and the normal section of maximum curvature ceases to be an arc of circle. The solution in this far region will not be discussed here.

The rise of the meniscus toward its equilibrium position (1) will be analyzed in what follows for $x = O(H_c)$ assuming that the motion of the liquid between the plates is dominated by viscosity. Under the action of the capillary depression Δp_s, the characteristic velocity of the liquid is then $v_c \sim \rho g H_c^2 \alpha^2/\mu$ from the balance of pressure and viscous forces $\Delta p_s/H_c \sim \mu v_c/(\alpha H_c)^2$. The effective Reynolds number measuring the effect of the inertia of the liquid (see, e.g., Ref. 38) is $\mathrm{Re} = \alpha^2\rho v_c H_c/\mu \sim \alpha^{5/2}\rho^{1/2}\sigma^{3/2}\cos^{3/2}\theta/g^{1/2}\mu^2$, which is assumed to be small. Lubrication theory[38] can then be used to compute the distribution of modified pressure P and the evolution of the meniscus. Here $P = p + \rho g z$, where p is the pressure of the liquid referred to the pressure of the surrounding gas (p_a) and z is the vertical distance from the level of the outer liquid. The intersection of the liquid surface with the symmetry plane bisecting the wedge is sought in the form $z = H(x,t)$. Scaling x, z, and H with H_c, P with $\rho g H_c$, and the time with $t_c = 12\mu/\rho g H_c \alpha^2$, the governing equations take the form

$$\frac{\partial}{\partial x}\left(x^3\frac{\partial P}{\partial x}\right) + x^3\frac{\partial^2 P}{\partial z^2} = 0 \quad \text{in} \quad 0 < z < H(x,t), \quad x > 0, \tag{2}$$

$$P = -\frac{1}{x} + H \tag{3a}$$

and

$$\frac{\partial H}{\partial t} - x^2\frac{\partial P}{\partial x}\frac{\partial H}{\partial x} + x^2\frac{\partial P}{\partial z} = 0 \tag{3b}$$

at $z = H(x,t)$,

$$P = 0 \quad \text{at} \quad z = 0, \tag{4}$$

$$x^3\frac{\partial P}{\partial x} \to 0 \quad \text{for} \quad x \to 0, \tag{5}$$

$$H \to 0 \quad \text{for} \quad x \to \infty. \tag{6}$$

Equation (2) is the Reynolds equation of lubrication theory for the modified pressure; i.e., the continuity equation $\nabla\cdot\boldsymbol{q} = 0$ for the Poiseuille flux $\boldsymbol{q} = -x^3\nabla P$. Equation (3a) expresses the condition that the modified pressure at the surface is the sum of the capillary depression $-\Delta p_s$ mentioned above, which is $-1/x$ in dimensionless variables, plus the gravity term H. Condition (3b) is an evolution equation for the meniscus, which is a material surface advancing with the width-averaged velocity of the local Poiseuille flow $\boldsymbol{v} = \boldsymbol{q}/x = -x^2\nabla P$. Condition (5) imposes that the flux through the edge of the wedge ($x = 0$) is zero. Problems (2), (3a), (3b), and (4)–(6) can be solved numerically for a given initial condition $H(x,0) = H_i(x)$ to describe the evolution toward the equilibrium solution $P = 0$, $H = H_e(x) = 1/x$.

III. ANALYSIS

If $H_i(x) = 0$, then the effect of the gravity is negligible in an early stage of the evolution in which $H \ll 1/x$. The solution in the absence of gravity is self-similar, of the form

$$P = \frac{1}{t}\hat{P}(\hat{x},\hat{z}), \quad H = t\hat{H}(\hat{x}), \quad \text{with} \quad \hat{x} = \frac{x}{t}, \quad \hat{z} = \frac{z}{t} \tag{7}$$

and

$$\frac{\partial}{\partial\hat{x}}\left(\hat{x}^3\frac{\partial\hat{P}}{\partial\hat{x}}\right) + \hat{x}^3\frac{\partial^2\hat{P}}{\partial\hat{z}^2} = 0 \quad \text{in} \quad 0 < \hat{z} < \hat{H}(\hat{x}), \quad \hat{x} > 0; \tag{8}$$

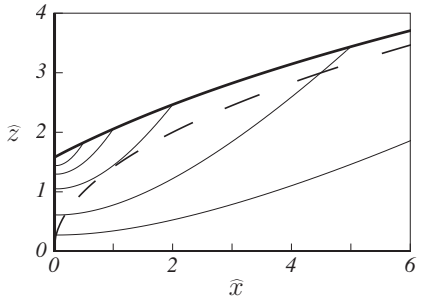

FIG. 2. Scaled height as a function of the scaled distance to the edge, $\hat{z}=\hat{H}(\hat{x})$ (solid, thick). The dashed curve is the asymptotic solution for large $\hat{x}$: $\hat{H}=(2\hat{x})^{1/2}$. The thin contours are isobars $\hat{P}=-2$, -1, -0.5, -0.2, and -0.08, from top to bottom.

$$\hat{P}=-\frac{1}{\hat{x}} \tag{9a}$$

and

$$\hat{H}-\hat{x}\hat{H}'-\hat{x}^2\frac{\partial\hat{P}}{\partial\hat{x}}\hat{H}'+\hat{x}^2\frac{\partial\hat{P}}{\partial\hat{z}}=0 \tag{9b}$$

at $\hat{z}=\hat{H}$;

$$\hat{P}=0 \quad \text{at } \hat{z}=0 \tag{10a}$$

and

$$\hat{x}^3\frac{\partial\hat{P}}{\partial\hat{x}}\to 0 \quad \text{for } \hat{x}\to 0, \tag{10b}$$

where $\hat{H}'=d\hat{H}/d\hat{x}$. A numerical solution of Eqs. (8), (9a), (9b), (10a), and (10b) has been computed using finite differences in the plane of the variables $\hat{x}$, $\hat{\eta}=\hat{z}/\hat{H}$. The scaled height $\hat{H}(\hat{x})$ and some isobars are shown in Fig. 2.

The point where the surface intersects the edge $\hat{x}=0$ is a singular point of Eqs. (8) and (9). The form of the solution in the vicinity of this point is as follows. Both $\hat{H}(\hat{x})$ and $\hat{H}'(\hat{x})$ tend to finite values $\hat{H}_0$ and $\hat{H}_0'$ for $\hat{x}\to 0$. The pressure for $(\hat{x},\hat{H}_0-\hat{z})\ll 1$ is of the form $\hat{P}=f(\varphi)/\hat{r}$, where $\hat{r}=[\hat{x}^2+(\hat{z}-\hat{H}_0)^2]^{1/2}$ and $\varphi=\arctan\hat{x}/(\hat{H}_0-\hat{z})$; see sketch on the left-hand side of Fig. 1. Here $f(\varphi)$ satisfies the equation $(\sin^3\varphi f')-2\sin^3\varphi f=0$ [from Eq. (8)] with the boundary conditions $f(\varphi_s)=-1/\sin\varphi_s$ and $\hat{H}_0+\sin\varphi_s f'(\varphi_s)=0$ at the surface [from Eqs. (9a) and (9b)], where $\varphi=\varphi_s=\pi/2+\arctan\hat{H}_0'$, and a condition of regularity at $\varphi=0$ to satisfy Eq. (10b). This latter condition rules out the singular solution of the equation for f, leaving only the regular solution (proportional to $f\sim 1+\varphi^2/4+\cdots$ for $\varphi\ll 1$) to satisfy the two boundary conditions at the surface. The whole local solution, including $f(\varphi)$ and $\hat{H}_0$, is therefore determined in terms of φ_s (hence $\hat{H}_0'$) only. The relation between $\hat{H}_0$ and $\hat{H}_0'$ determined by this local analysis is shown in Fig. 3. The value of $\hat{H}_0$ must be independently determined from the numerical solution of Eqs. (8), (9a), (9b), (10a), and (10b) shown in Fig. 2. A finite $\hat{H}_0$ means that the height of the surface at the edge increases proportionally to time in the absence of gravity,

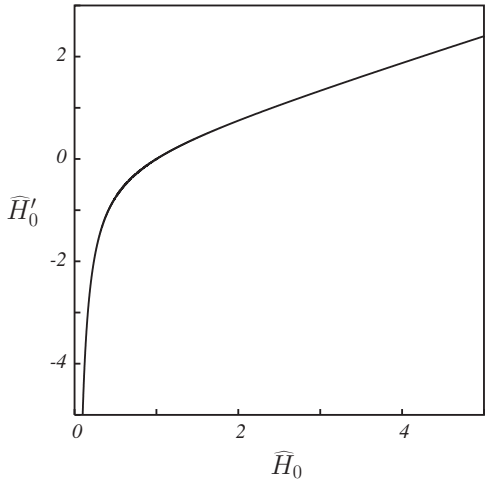

FIG. 3. Relation between $\hat{H}_0$ and $\hat{H}_0'$ (or between $\partial H/\partial t$ and $\partial H/\partial x$ at $x=0$).

which is in agreement with the results of Fig. 5(b) below for small times. The local analysis carried out here is also applicable to problem (2)–(6) for $(x,H(0,t)-z)\ll 1$ and any t because the effect of gravity [last term on the right-hand side of Eq. (3a)] is negligible for $x\ll 1$. The result of Fig. 3 is still valid with $\partial H/\partial t$ and $\partial H/\partial x$ at $x=0$ playing the roles of $\hat{H}$ and $\hat{H}'$. Figure 5(b) below shows that $\partial H/\partial t|_{x=0}$ decreases with time during the rise of the liquid, and so does $\partial H/\partial x|_{x=0}$, which changes from positive to negative at a certain time [see Fig. 5(a)].

For $\hat{x}\gg 1$, Eq. (8) reduces to $\partial^2\hat{P}/\partial\hat{z}^2\approx 0$, whose solution with the boundary conditions (9a) and (10a) is $\hat{P}=-\hat{z}/(\hat{x}\hat{H})$. Carrying this pressure to Eq. (9b), the term $-\hat{x}^2\hat{H}'\,\partial\hat{P}/\hat{x}$ can be seen to be negligible, and the balance of the other three terms gives $\hat{H}=(2\hat{x})^{1/2}$. This result reads as $H=(2xt)^{1/2}$ in the original variables, which amounts to Washburn's[39] classical square root penetration law in a channel of width equal to the local distance between the plates. In the absence of gravity, the penetration rate increases with the square root of the distance to the edge x because the decrease in the hydraulic resistance with increasing x overcomes the decrease in the capillary depression at the surface.

As time goes on, gravity first checks the $H\sim(2xt)^{1/2}$ penetration law at large distances from the edge. The condition $(2xt)^{1/2}\sim H_e=1/x$ gives the characteristic time of rise of the meniscus to its equilibrium position as $t\sim 1/x^3$, so that the meniscus may be nearly at equilibrium far from the edge when it is still rising nearer to the edge.

We turn now to problem (2)–(6). Since $H\ll 1$ for small times, Eq. (2) can be approximated by $\partial^2 P/\partial z^2=0$ for $t\ll 1$ at any $x\gg H$. Proceeding as before but with the last term of Eq. (3a) retained, Eq. (3b) can be seen to reduce to $\partial H/\partial t=(1-xH)x/H$, which means that the meniscus rises independently for different values of x. The solution of this equation with the initial condition $H_i=0$ is

$$xH+\ln(1-xH)=-x^3t, \tag{11}$$

which is shown in Fig. 4 for different values of t. The height $H(x,t)$ has a maximum, $H_{\max}\approx 0.882t^{1/3}$, at $x=x_{\max}\approx 0.731/t^{1/3}$.

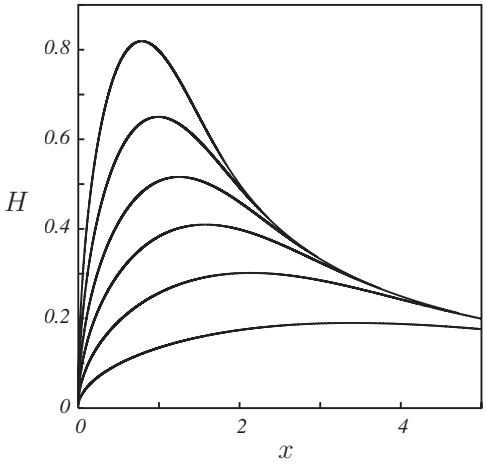

FIG. 4. Height of the liquid as a function of x for $t=0.01$, 0.04, 0.1, 0.2, 0.4, and 0.8, increasing from bottom to top, from the solution (11) for small times.

A numerical solution of Eqs. (2), (3a), (3b), and (4)–(6) has been computed using Eq. (11) as an initial condition at a small value of t. The distribution of $H(x,t)$ is shown in Fig. 5(a) for various times. As can be seen, the maximum height keeps increasing with time and shifting toward the edge, which it reaches in a finite time. The subsequent evolution leads to a layer of liquid around the edge which continuously elongates and thins, and leaves the meniscus nearly at equilibrium outside of this layer.

To describe the asymptotic solution in the thin layer for large values of the dimensionless time, it is convenient to seek the position of the meniscus in the alternative form $x=G(z,t)$. Conditions (3) become

$$P=-\frac{1}{G}+z \tag{12a}$$

and

$$\frac{\partial G}{\partial t}+v_z\frac{\partial G}{\partial z}-v_x=0 \tag{12b}$$

at $x=G(z,t)$, where $v_x=q_x/x=-x^2\partial P/\partial x$ and $v_z=q_z/x=-x^2\partial P/\partial z$. Equation (2) requires that $P=P(z,t)$ in first approximation in the thin layer. Condition (12a) then gives $P(z,t)=-1/G(z,t)+z$, and therefore, $q_z=-x^3\partial P/\partial z=-x^3(1+G^{-2}\partial G/\partial z)$. Equation (2) written in the form $\partial q_x/\partial x+\partial q_z/\partial z=0$ can now be integrated with the boundary condition (5) to give

$$q_x=-\int_0^x\frac{\partial q_z}{\partial z}dx=\frac{x^4}{4}\frac{\partial}{\partial z}\left(\frac{1}{G^2}\frac{\partial G}{\partial z}\right).$$

Using these q_x and q_z to evaluate v_x and v_z in Eq. (12b), this equation becomes

$$\frac{\partial G}{\partial t}-\left(G^2+\frac{1}{2}\frac{\partial G}{\partial z}\right)\frac{\partial G}{\partial z}=\frac{1}{4}G\frac{\partial^2 G}{\partial z^2}. \tag{13}$$

Equations similar to Eq. (13) have been found in a number of related problems (see, e.g., Refs. 19–31 and references therein). Equation (13) admits solutions with $G=0$ beyond an advancing front. For large t, these solutions tend to become self-similar, of the form $G=\tilde{G}(\tilde{z})/t^{1/3}$ with $\tilde{z}=z/t^{1/3}$ and $\frac{1}{4}\tilde{G}\tilde{G}''+\left(\tilde{G}^2+\frac{1}{2}\tilde{G}'\right)\tilde{G}'+\frac{1}{3}(\tilde{z}\tilde{G})'=0$. This equation for $\tilde{G}$ must be solved with the conditions $\tilde{G}\to 1/\tilde{z}$ for $\tilde{z}\to 0$ and $\tilde{G}=\frac{2}{3}\tilde{z}_0(\tilde{z}_0-\tilde{z})$ for $0<(\tilde{z}_0-\tilde{z})\ll 1$ at a certain z_0. From its numerical solution, $\tilde{z}_0\approx 1.81$. The $t^{1/3}$ elevation of the meniscus at the edge predicted by the self-similar solution is realized by the numerical solution of Fig. 5(b) for large values of t.

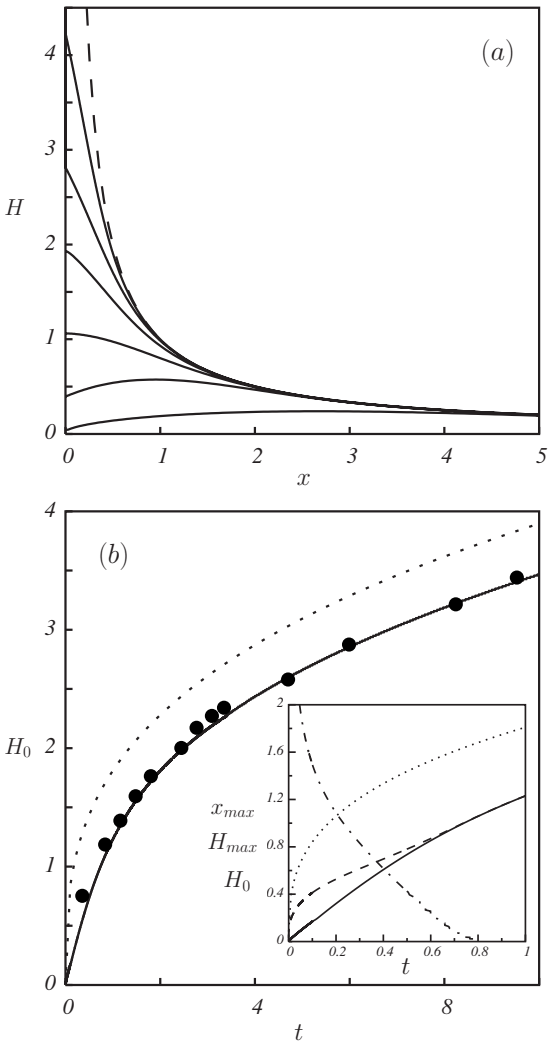

FIG. 5. (a) Distributions of height at $t=0.02$, 0.252, 0.802, 2.302, 3.8, and 12.8, increasing from bottom to top. The dashed curve is the equilibrium distribution $H_e=1/x$. (b) Height at the edge [$H_0=H(x=0,t)$, solid], maximum height (H_{max}, dashed), and position of maximum height (x_{max}, dot-dashed) as functions of time. The dotted curve is the asymptote $H=1.81t^{1/3}$. Circles are experimental values of H_0.

IV. EXPERIMENT

Two square plates of glass 20×20 cm^2 in size are set at an angle of 1.25° by keeping them in contact along a vertical edge and introducing spacers at the opposite edge. The lower edges of the plates are gently introduced in silicone oil with viscosity of 460 cP (density $\rho=971$ kg m^{-3}, surface tension $\sigma=2.1\times 10^{-2}$ N m^{-1}, Dow Corning) which wets the plates and rises between them. The meniscus is illuminated from a side of the plates through a translucent screen and photo-

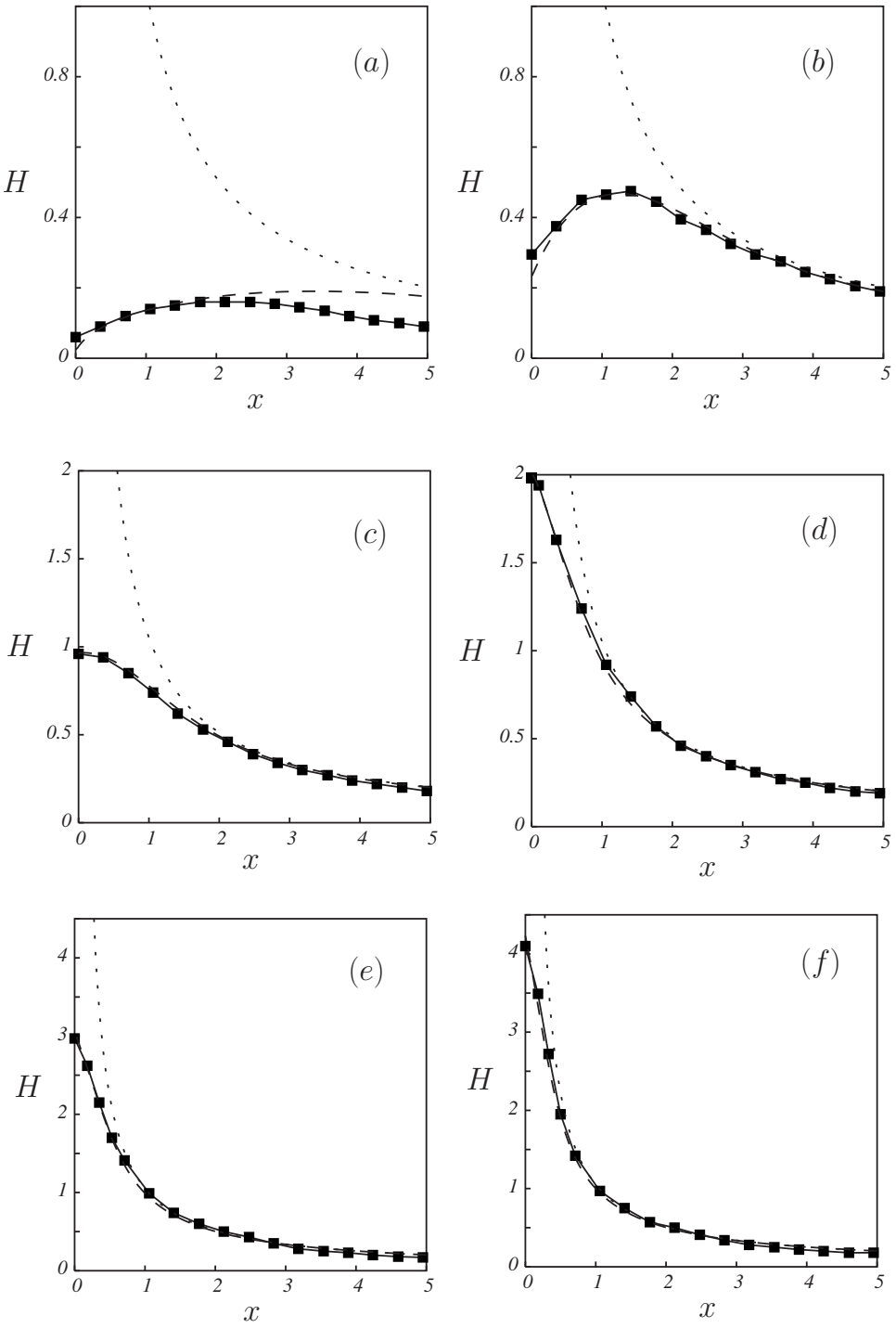

FIG. 6. Experimental distributions of dimensionless height at $t=0.04$ (a), 0.22 (b), 0.72 (c), 2.08 (d), 6.33 (e), and 12.70 (f). The dashed curves are numerical results for the same dimensionless times. In each panel, the dotted curve shows the equilibrium distribution $H_e=1/x$.

graphed with a camera set opposite to the light source at the other side of the plates. The camera is periodically triggered at a selected frequency. The spacers are disks of known size and thickness, whose images serve to fix the length scale on the photographs.

Following Ferguson and Vogel[40] and Lopez de Ramos and Cerro,[41] the value of H_c in Eq. (1) is determined directly from the final equilibrium meniscus as the common value of the height and the distance to the edge of the point on the hyperbola where its slope is equal to unity. This procedure does not require an independent determination of the contact angle θ. We find $H_c \approx 14.14$ mm from the photographs for very large times. Using this H_c, the value of t_c defined above Eq. (2) is $t_c \approx 86.10$ s for the experiment.

Figure 6 shows a sequence of distributions of the liquid height extracted from the photographs at different instants of time. Distances and times are nondimensionalized with H_c and t_c. The height of the liquid is maximum at a point away from the common edge of the plates during a first stage of the process. With time, the maximum height increases and the point where the maximum is attained approaches the edge. In the second stage, the maximum height occurs at the edge and keeps increasing with time, while the height away from the edge stabilizes at the equilibrium hyperbola. The

circles in Fig. 5(b) show the measured height at the edge as a function of time. As can be seen, the numerical results of Sec. III are in good agreement with the experimental data of Figs. 5(b) and 6. The largest discrepancies occur at the beginning of the process [Fig. 6(a)], which may be due to several reasons. First, the lubrication approximation is not valid at these small times because the height of the liquid is not large compared to the local spacing of the plates. Second, the accuracy of the measurements on the photographs is low when the image of the liquid surface between the plates is close to the dark image of the menisci at the outer sides of the plates. In addition, the rise of the liquid may begin at slightly different times at different points along the lower edges depending on how the plates are introduced in the liquid.

V. CONCLUSIONS

The time evolution of the meniscus of a wetting liquid in the gap between two vertical plates making a small angle has been computed assuming that the motion of the liquid is dominated by viscous forces. In the first stage of evolution, the effect of the gravity is negligible in a region around the edge of the gap where the height of the liquid increases proportionally to time. The maximum height, however, is proportional to the cubic root of time and is attained outside of this region, at a distance from the edge inversely proportional to the cubic root of time. The point of maximum height reaches the edge at a finite time during the evolution. At later times, a thin layer develops around the edge where the flow is nearly vertical and outside which the meniscus is nearly at equilibrium. The layer becomes self-similar for large times, with a height that increases as the cubic root of time and a thickness that decreases as the inverse of this quantity. A simple experiment has been conducted in which the rise of silicone oil between two glass plates is photographically recorded. The computed evolution is in good agreement with the experimental results.

ACKNOWLEDGMENTS

This work was supported by the Spanish Ministerio de Educación y Ciencia through Project No. DPI2007-66659-C03-02.

[1] S. F. Kistler, in *Hydrodynamics of Wetting*, Wettability, Surfactant Science Series Vol. 49, edited by J. C. Berg (Dekker, New York, 1993), p. 311.
[2] P. H. Steen, in *Capillarity and Interfacial Phenomena, Wetting and Spreading*, Research Trends in Fluid Mechanics, edited by J. L. Lumley, A. Acrivos, L. G. Leal, and S. Leibovich (AIP, New York, 1996), pp. 286–295.
[3] B. Taylor, "Concerning the ascent of water between two glass plates," Philos. Trans. R. Soc. London **27**, 538 (1712).
[4] F. Hauksbee, "An experiment touching the ascent of water between two glass plates in an hyperbolick figure," Philos. Trans. R. Soc. London **27**, 539 (1712).
[5] P. Concus and R. Finn, "On the behavior of a capillary free surface in a wedge," Proc. Natl. Acad. Sci. U.S.A. **63**, 292 (1969).
[6] G. Mason and N. Morrow, "Capillary behavior of a perfectly wetting liquid in irregular triangular tubes," J. Colloid Interface Sci. **141**, 262 (1991).
[7] D. Langbein, "The shape and equilibrium of liquid menisci at solid edges," J. Fluid Mech. **213**, 251 (1990).
[8] H. Wong, S. Morris, and C. J. Radke, "Three-dimensional menisci in polygonal capillaries," J. Colloid Interface Sci. **148**, 317 (1992).
[9] P. M. Heertjes and W. C. Witveet, "Some aspects of the wetting of powders," Powder Technol. **3**, 339 (1970).
[10] O. Vizika and A. C. Payatakes, "Parametric experimental study of forced imbibition in porous media," PCH, PhysicoChem. Hydrodyn. **11**, 787 (1989).
[11] J. L. Wilson, S. H. Conrad, E. Hagan, W. R. Mason, and P. Peplinski, in *The Pore Level Spatial Distribution and Saturation of Organic Liquids in Porous Media*, Proceedings of the NWWA/API Conference on Petroleum Hydrocarbons in Ground Water, Houston, TX (National Water Well Association, Dublin, OH, 1988), pp. 107–133.
[12] J. B. Grotberg, "Pulmonary flow and transport phenomena," Annu. Rev. Fluid Mech. **26**, 529 (1994).
[13] J. Rosenzweig and O. E. Jensen, "Capillary-elastic instabilities of liquid-lined lung airways," J. Biomech. Eng. **124**, 650 (2002).
[14] H. Wong, I. Fatt, and C. J. Radke, "Deposition and thinning of the human tear film," J. Colloid Interface Sci. **184**, 44 (1996).
[15] J. A. Moriarty and E. L. Terrill, "Mathematical modelling of the motion of hard contact lenses," Eur. J. Appl. Math. **7**, 575 (1996).
[16] T. G. Myers, "Unsteady laminar flow over a rough surface," J. Eng. Math. **46**, 111 (2003).
[17] L. W. Schwartz and D. E. Weidner, "Modeling of coating flows on curves surfaces," J. Eng. Math. **29**, 91 (1995).
[18] R. Lenormand and C. Zarcone, "Role of Roughness and Edges During Imbibition in Square Capillaries," Proceedings of the 59th Annual Meeting of the SPE, Houston, TX (Society of Petroleum Engineers, Dallas, 1984), SPE Paper No. 13264.
[19] P. S. Ayyaswamy, I. Catton, and D. K. Edwards, "Capillary flow in triangular grooves," Trans. ASME, J. Appl. Mech. **41**, 332 (1974).
[20] T. C. Ransohoff and C. J. Radke, "Laminar flow of a wetting liquid along corners of a predominantly gas-occupied noncircular pore," J. Colloid Interface Sci. **121**, 392 (1988).
[21] M. Dong and I. Chatzis, "The imbibition and flow of a wetting liquid along the corners of a square capillary tube," J. Colloid Interface Sci. **172**, 278 (1995).
[22] M. M. Weislogel and S. Lichter, "Capillary flow in an interior corner," J. Fluid Mech. **373**, 349 (1998).
[23] M. M. Weislogel, "Capillary flow in interior corners: The infinite column," Phys. Fluids **13**, 3101 (2001).
[24] G. Verbist, D. Weaire, and A. M. Kraynik, "The foam drainage equation," J. Phys.: Condens. Matter **8**, 3715 (1996).
[25] A. R. Kovcek and C. J. Radke, "Gas bubble snap-off under pressure-driven flow in constricted noncircular capillaries," Colloids Surf., A **117**, 56 (1996).
[26] H. B. Ma, G. P. Peterson, and X. Lu, "The influence of vapor-liquid interactions on the liquid pressure drop in triangular microgrooves," Int. J. Heat Mass Transfer **37**, 2211 (1994).
[27] G. P. Peterson and H. B. Ma, "Analysis of countercurrent liquid-vapor interactions and the effect on the liquid friction factor," Exp. Therm. Fluid Sci. **12**, 13 (1996).
[28] H. B. Ma and G. P. Peterson, "Laminar friction factor in micro-scale ducts of irregular cross section," Microscale Thermophys. Eng. **1**, 253 (1997).
[29] G. P. Peterson and H. B. Ma "Theoretical analysis of the maximum heat transport in triangular grooves: A study of idealized micro heat pipes," J. Heat Transfer **118**, 731 (1996).
[30] H. B. Ma and G. P. Peterson, "Temperature variation and heat transfer in triangular grooves with an evaporating film," J. Thermophys. Heat Transfer **11**, 90 (1997).
[31] S.-K. Su and C.-L. Lai, "Interfacial shear-stress effects on transient capillary wedge flows," Phys. Fluids **16**, 2033 (2004).
[32] W. B. Kolb and R. L. Cerro, "The motion of long bubbles in tubes of square cross section," Phys. Fluids A **5**, 1549 (1993).
[33] J. Bico and D. Quéré, "Rise of liquids and bubbles in angular capillary tubes," J. Colloid Interface Sci. **247**, 162 (2002).
[34] M. M. Weislogel, "Some analytical tools for fluid management is space: Isothermal capillary flows along interior corners," Adv. Space Res. **32**, 163 (2003).
[35] J. A. Mann, L. Romero, R. R. Rye, and F. G. Yost, "Flow of simple liquids down narrow V grooves'," Phys. Rev. E **52**, 3967 (1995).
[36] P. Warren, "Late stage kinetics for various wicking and spreading problems," Phys. Rev. E **69**, 041601 (2004).
[37] R. Stocker and A. E. Hosoi, "Lubrication in a corner," J. Fluid Mech. **544**, 353 (2005).

[38]G. K. Batchelor, *An Introduction to Fluid Dynamics* (Cambridge University Press, Cambridge, England, 1967).
[39]E. W. Washburn, "The dynamics of capillary flow," Phys. Rev. **17**, 273 (1921).
[40]A. Ferguson and I. Vogel, "On the 'hyperbola' method for the measurement of surface tension," Proc. Phys. Soc. London **38**, 193 (1925).
[41]A. Lopez de Ramos and R. L. Cerro, "Liquid filament rise in corners of square capillaries: A novel method for the measurement of small contact angles," Chem. Eng. Sci. **49**, 2395 (1994).